THE JOURNAL OF PHYSICAL CHEMISTRY Letters

Letter

pubs.acs.org/JPCL

Direct In Situ Quantification of HO_2 from a Flow Reactor

Brian Brumfield,[†] Wenting Sun,[‡] Yiguang Ju,*[,‡] and Gerard Wysocki*[,†]

[†]Department of Electrical Engineering and [‡]Department of Mechanical and Aerospace Engineering, Princeton University, Engineering Quadrangle, Princeton, New Jersey 08544, United States

Supporting Information

ABSTRACT: The first direct in situ measurements of hydroperoxyl radical (HO_2) at atmospheric pressure from the exit of a laminar flow reactor have been carried out using mid-infrared Faraday rotation spectroscopy. HO_2 was generated by oxidation of dimethyl ether, a potential renewable biofuel with a simple molecular structure but rich low-temperature oxidation chemistry. On the basis of the results of nonlinear fitting of the experimental data to a theoretical spectroscopic model, the technique offers an estimated sensitivity of <1 ppmv over a reactor exit temperature range of 398−673 K. Accurate in situ measurement of this species will aid in quantitative modeling of low-temperature and high-pressure combustion kinetics.

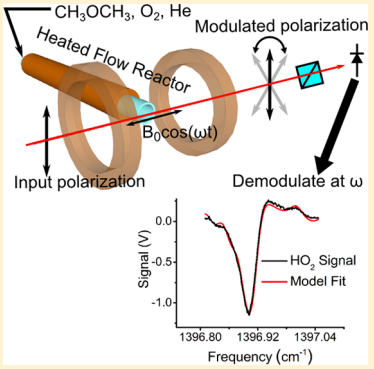

SECTION: Spectroscopy, Photochemistry, and Excited States

With increasing concerns of energy sustainability and renewability, future internal combustion engines need to be designed for operation at higher pressures and lower temperatures to achieve higher fuel efficiency, lower emissions, and greater fuel flexibility.[1] An accurate prediction of the combustion chemistry under these conditions using detailed chemical kinetic models is critical to achieve this goal.[2] Under these physical conditions, H_2O_2 and HO_2 play key roles in the fuel oxidation chemistry and the autoignition process. However, these chemical species remain difficult to quantify in experiments, leaving large uncertainties in chemical kinetic models. In this work, we use mid-infrared Faraday rotation spectroscopy (FRS) to perform the first direct in situ quantification of the HO_2 radical at atmospheric pressure during low-temperature oxidation of dimethyl ether in a laminar flow reactor.

Figure 1 presents the important reaction pathways that describe the oxidation of hydrocarbon fuels. The scheme begins with the formation of an alkyl radical through a H abstraction reaction of the fuel (RH) by OH. At low (below 900 K) and intermediate temperatures (900−1200 K), HO_2 radicals are formed from reactions of R with O_2, with a subsequent reaction of HO_2 with RH and O_2 leading to the formation of H_2O_2. The decomposition of H_2O_2 to OH is the governing branching reaction that leads to "hot ignition".[2] At high pressure, HO_2 + H = 2OH is another important branching reaction at high temperature. Therefore, the formation and consumption of HO_2 and H_2O_2 are important in high-pressure combustion kinetics for all fuels from hydrogen[3] to large hydrocarbons and biofuels.[2] Direct measurements of these two species in high-pressure combustion are extremely challenging, leading to large uncertainties in chemical kinetic models. Recently, direct measurements of H_2O_2 were conducted by using molecular beam mass spectrometry[4,5] (MBMS) at 1 atm and cavity ring-down spectroscopy (cw-CRDS)[6] at 0.01 atm. However, both methods required intrusive sampling, which causes uncertainty due to wall quenching. The wall quenching problem has recently been blamed for the failure in detection of HO_2 from a jet-stirred reactor using near-IR cw-CRDS.[7]

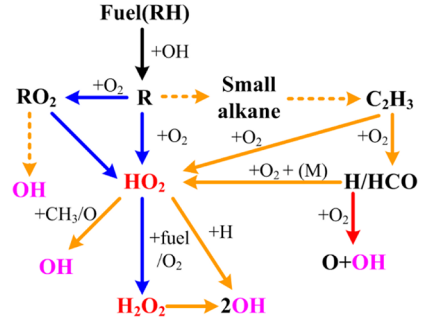

Figure 1. A schematic of the key reaction pathways for oxidation of hydrocarbon fuels at high pressure (blue arrows: low temperature; yellow arrows: intermediate temperature; red arrow: high temperature; dotted arrows: many elementary steps).

Recently, Hong et al.[8] investigated the relative evolution of HO_2 by using absorbance at 227 nm in a shock tube. However, this method relies on the accuracy of a kinetic mechanism that may not be well validated at high pressure. The UV absorption is also complicated by spectral interference from H_2O_2 and large hydrocarbon molecules. Spectral interference is also a

Received: January 21, 2013
Accepted: February 27, 2013
Published: February 27, 2013

problem that is encountered for near-IR optical detection of HO_2, particularly at high pressure.[7,9]

In contrast to optical absorption methods, FRS is a dispersion-based magneto-optical technique that is selective only to paramagnetic (radical) species. Signals from diamagnetic molecules, such as H_2O, are suppressed, which significantly mitigates the problem of spectral interference. In theory, FRS is a zero-background technique with a distinct advantage over absorption spectroscopy as a combustion diagnostic for small gas-phase radicals (i.e., OH, NO, NO_2, HCO). Larger paramagnetic species with more congested spectra increase the chance for FRS signal cancellation due to adjacent transitions of the same molecule with an opposite response to the applied magnetic field.

In FRS, a longitudinal magnetic field is applied to a sample containing paramagnetic species. This induces magnetic circular birefringence in the vicinity of spectral transitions belonging to the paramagnetic species causing polarization rotation in the transmitted radiation (the Faraday effect). The amount of polarization rotation depends on the strength of the applied magnetic field, the transition intensity, and the number density of the paramagnetic species. Due to the latter, FRS can be used for concentration measurements of radical species.

In a typical FRS experimental setup, linearly polarized laser light with a well-defined polarization axis is passed through the sample located within a longitudinal magnetic field. The polarization rotation of the transmitted light is transformed into intensity variations using a polarizer (polarization analyzer). The FRS signal encoded in the light intensity can then be measured with a photodetector. To suppress the noise and enhance the detection sensitivity, an oscillating magnetic field is applied to the sample, and the FRS signal is demodulated as a harmonic of the modulation frequency using narrow-band phase-sensitive lock-in detection.

The FRS experiment shown in Figure 2 was designed to measure HO_2 at the exit of an atmospheric flow reactor. An external cavity quantum cascade laser (EC-QCL, Daylight Solutions, model 21074-MHF) operating in continuous wave (CW) mode was used to provide tunable light for probing the HO_2 Q-branch transitions in the ν_2 bending fundamental at around 1400 cm^{-1} (7.1 μm). The first polarization element before the sample is a wedged Ge window at the Brewster's angle. Light reflected off of the window is then passed three times within a plane 2 mm from the flow reactor exit using a pair of bare gold-coated mirrors. This provides a 5 cm optical path through the sample. A longitudinal magnetic field (125 G RMS) oscillating at 610 Hz is generated in the sampling region using a Helmholtz coil. The transmitted light passes through the polarization analyzer and is focused onto a photodetector (Vigo PVI-4TE-8). The output signal from the photodetector is demodulated using a lock-in amplifier (Signal Recovery Model 7265). Two wire grid polarizers with a combined extinction ratio of 10 000:1 were used as a polarization analyzer. After analysis of the system noise, the signal-to-noise ratio (SNR) was maximized by offsetting the polarization axes of both wire grid polarizers by an optimum angle of 0.80° from a fully crossed position. The reflected light from the first wire grid polarizer is directed to a wavemeter (Bristol Instruments Model 721) for frequency calibration.

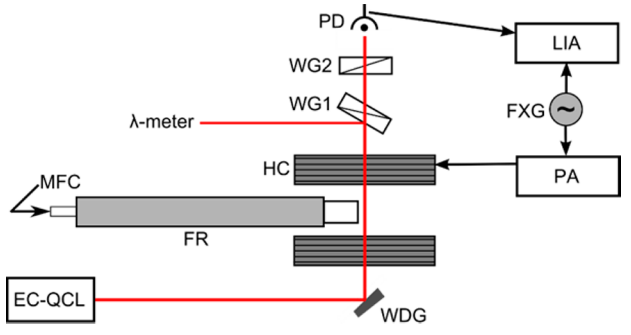

Figure 2. Experimental layout of the FRS system for in situ detection of HO_2 in a flow reactor. The setup consists of (EC-QCL) a laser, (WDG) a germanium wedge used as a reflective polarization element, (HC) Helmholtz coils, (FR) a flow reactor, (MFC) mass flow controllers, (λ-meter) a wavemeter, (WG1,2) wire grid polarizer #1 and #2, (PD) a photodetector, (LIA) a lock-in amplifier, (PA) a power amplifier, and (FXG) a function generator.

The flow reactor is made of a quartz tube (355 mm in length, 17 mm in diameter) surrounded by a copper sleeve heated by resistive wire. The temperature inside of the flow reactor is monitored using a thermocouple. Mass flow controllers are used to control the concentrations and adjust the residence time of He, O_2, and dimethyl ether (DME) in the gas mixture introduced into the flow reactor. A mixture of ~90% He, ~10% O_2, and ~1% DME was used at a total flow rate that provides a 0.35 s residence time in the reactor for all experimental data presented. The experiments were conducted at atmospheric pressure.

On the basis of spectroscopic modeling using parameters from the HITRAN database,[10] an HO_2 spectral feature composed of multiple Q-branch transitions with a peak signal at 1396.90 cm^{-1} was selected as the target.

The signal modeling takes into account system parameters to calculate the laser-frequency-dependent RMS signal voltage (V_{RMS}) at the output of the detector

$$V_{RMS}(\tilde{\nu}) = GP_0 \sin 2\theta\, \Theta_{RMS}(\tilde{\nu})$$

where G is an experimental factor that combines the transmission through the wire grid polarizers, the gain of the lock-in amplifier, the detector gain, and the optical collection efficiency at the detector. The optical power incident on the wire grid polarizer is given by P_0, and the polarization analyzer offset angle is given by θ. $\Theta_{RMS}(\tilde{\nu})$ is the root-mean-square value for the Faraday rotation angle as a function of optical frequency.

The Θ_{RMS} spectrum is calculated for individual HO_2 transitions at discrete frequency points over the spectral window by numerically calculating the first Fourier component at the magnetic field modulation frequency. A detailed discussion of the method for calculating $\Theta_{RMS}(\tilde{\nu})$ is beyond the scope of the current Letter, but it has been extensively discussed in the literature (e.g., see Westberg et al.[11]). Figure 3a shows that the target spectral feature is composed of 13 HO_2 transitions. The HITRAN line intensities are scaled for the expected sample temperature using a polynomial expression for the total internal partition function sum.[12] The model used for spectral fitting requires the following input parameters: the RMS value of the magnetic field, the temperature of the gas sample at the reactor exit, and the optical path length. Four parameters in the model were used as variables, the HO_2 number density (n_{HO_2}), the collision-broadened line width ($\Delta\tilde{\nu}_{HWHM}$), a signal offset, and a frequency offset. The signal and frequency offsets have been implemented to account for

dx.doi.org/10.1021/jz400143c | J. Phys. Chem. Lett. 2013, 4, 872−876

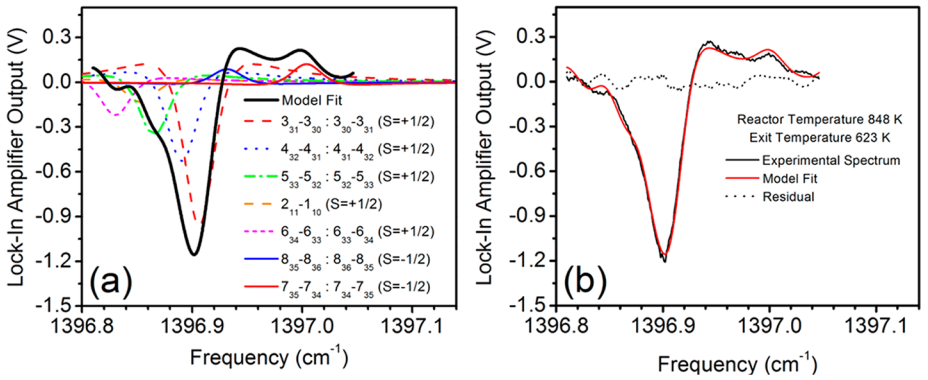

Figure 3. (a) The target HO_2 FRS feature modeled using the HITRAN database parameters. Asymmetric top notation ($N_{Ka, Kc}$) is used to label the individual transitions in the legend. The sign of the electron spin shared by the final and initial states for each transition is provided in the parentheses of the legend. (b) A comparison between the experimentally observed FRS signal at a flow reactor temperature of 848 K and the resulting model fit at an average reactor exit temperature of 623 K.

systematic errors due to electromagnetic interference (EMI) from the Helmholtz coils and an offset of the wavemeter frequency reading, respectively. $\Delta\tilde{\nu}_{HWHM}$ is a fitted parameter because the collisional broadening for HO_2 is unknown for gas mixtures composed of 90% He and 10% O_2 at 1 atm pressure. A nonlinear least-squares fitting algorithm has been implemented to find the best fit and determine the HO_2 number density (n_{HO_2}) in the sample.

It should be noted that the spectroscopic model predicts a reduction in the FRS signal as a function of pressure for a fixed HO_2 concentration and magnetic field strength. The FRS signal depends on the Zeeman splitting provided with the magnetic field and the collisional line broadening. The optimum signal is generated when the Zeeman splitting of the $\Delta m = +1$ and -1 components are separated by the fwhm of the transition. At atmospheric pressure, a magnetic field of >1 kG is required for optimal Zeeman splitting. Generating an AC magnetic field this large is technically challenging, and as a result, the Zeeman splitting is always far below optimum. Because of these effects, modeling indicates that an increase in the sample pressure from 1 to 4 atm will result in a 10-fold decrease in the FRS signal that will reduce the minimum detection limit. However, chemical kinetic models predict an increase in HO_2 formation at higher pressures, which is expected to partially compensate for this reduction in sensitivity, yielding comparable SNR for the measurement.

The FRS spectrum recorded at 1396.90 cm^{-1} is shown in Figure 3b. The spectrum was acquired by step scanning of the EC-QCL, and the signal offset has been corrected in the postprocessing of the data. A 2 s lock-in amplifier time constant was used, and each spectral data point was acquired with a 6 s delay between EC-QCL laser frequency steps. With all additional operations included (e.g., wavemeter reading time delay), a spectrum with 220 spectral points required an acquisition time of roughly 30 min.

The long acquisition time arises from the narrow detection bandwidth that must be used to suppress the high experimental 1/f noise observed due to the relatively low modulation frequency of the magnetic field. For a single spectral point, a SNR of 45:1 is estimated by comparing the peak-to-peak signal amplitude to the standard deviation of the residuals from the model fit. It should be noted that the spectral fitting uses multiple spectral points, which effectively improves the sensitivity, and in our case, the relative uncertainty in the HO_2 concentrations obtained from the spectral fitting is below 1%. However, for further discussion, we will use the single spectral point SNR, which is a conservative approximation that also includes small discrepancies between the spectroscopic model and the experimental signal. The structure in the fitting residuals occurs due to uncertainties in the available molecular parameters used in the model fitting combined with residual optical fringing that is not entirely suppressed in the spectrum. Fringing in the FRS spectrum is present because of unwanted electromagnetic pickup. The effectiveness of the background subtraction can be observed for data in the Supporting Information.

There is excellent agreement between the experimental data and the fitted model of the FRS spectrum, as shown in Figure 3b. An n_{HO2} of 6.6×10^{13} cm^{-3} (5.6 ppmv) was calculated at an average reactor exit temperature of 623 K. The exit temperature used in the model fit was 225 K less than the center temperature of the flow reactor. The exit temperature used in the modeling is the average of the axial and radial temperature gradients that were experimentally measured using a thermocouple probe. The spectroscopic model assumes this average temperature and a uniform concentration across the region of the reactor exit sampled by the laser beam. This will be verified in the future by implementing spatially resolved measurements by translating the flow reactor or the laser beam.

At these conditions, the single spectral point SNR of 45:1 yields a 1σ concentration detection limit of 0.1 ppmv (or n_{HO_2-min} of 1.5×10^{12} cm^{-3}). For comparison with conventional absorption spectroscopy methods in the mid-IR, this corresponds to a bandwidth-normalized fractional absorption sensitivity of 5×10^{-7} $Hz^{-1/2}$ (also estimated for a single spectral point). There are spectral regions of the ν_2 band with minimal interference from water absorption, including the currently targeted spectral feature. Given the best reflectivity of commercially available dielectric mirrors ($R = 0.9998$) near this spectral region and assuming the performance of previously reported QCL-based cw-CRDS,[13] an HO_2 detection limit of 0.01 ppmv (1.2×10^{11} cm^{-3}) is theoretically achievable at the experimental conditions used in this work. In practice, the actual sensitivity for mid-IR CRDS will suffer due to beam deflection caused by temperature gradients at the exit of the flow reactor and broad-band absorption from other species (i.e., H_2O),[14,15] resulting in a sensitivity that is on the same level as that of the current FRS prototype. Further optimization of the

dx.doi.org/10.1021/jz400143c | J. Phys. Chem. Lett. 2013, 4, 872−876

FRS system is possible and will be discussed in the concluding paragraphs.

The FRS signal from the spectral feature at 1396.90 cm^{-1} was monitored over a series of flow reactor temperatures ranging from 523 to 923 K. A plot of the retrieved HO_2 concentration as a function of temperature is shown in Figure 4. The experimental data, spectral fits, and residuals for each

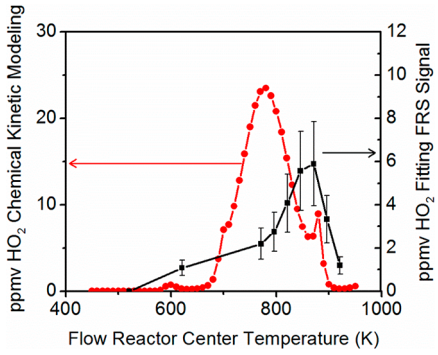

Figure 4. The HO_2 concentration versus flow reactor temperature for data obtained from chemical kinetic modeling (red) and concentration data retrieved from the FRS spectra (black). The 1σ error bars for the concentration estimates from the spectral fitting are based on the combined relative uncertainties from the HITRAN line intensities and experimental parameters.

data point are provided as Supporting Information. For experimental measurements acquired over average temperatures between 398 and 673 K at the reactor exit, the 1σ detection limit gradually increases from 0.03 to 0.17 ppmv. This increase agrees with the temperature dependence of the partition function for HO_2. A temperature-independent value of the pressure-broadening coefficient of 0.0286 ± 0.006 cm^{-1}/atm was found across all of the measurements. The observed temperature independence of the pressure-broadening coefficient arises from the significant spectral overlap between multiple transitions. The average value is within 20% of the He pressure broadening obtained by near-IR measurements of HO_2 at 296 K.[16,17]

The maximum relative uncertainty in the HO_2 concentrations obtained as the fitting error is ~1%. This level of fit uncertainty is negligible compared to other sources of error such as the uncertainties in the line intensities used in the spectroscopic model or experimental parameters. The line intensities from HITRAN are obtained from an experimental measurement of the ν_2 band strength with a 28% relative uncertainty.[18] The largest experimental error is from the 20% uncertainty in the detector response. This results in a combined relative uncertainty of 33% for the HO_2 concentrations, and this is shown with error bars in Figure 4.

The experimental measurements of the HO_2 concentration shown in Figure 4 have been plotted against concentration estimates derived by chemical kinetic modeling. The chemical kinetic modeling has been performed numerically using a zero-dimensional flow reactor. Due to the heat loss to the environment, the temperature profiles were not uniform. The numerical simulations were conducted using the temperature profile measured with a thermocouple along the axis of the reactor to compensate for the uncertainty caused by temperature gradients. The modeling results were obtained using SENKIN[19] with a chemical kinetic model for DME oxidation created by Zhao et al.[20]

There are significant differences in the HO_2 concentration profiles obtained from the FRS measurement and from the chemical kinetic model. Both the measurement and the kinetic modeling show a distinct peak in the HO_2 concentrations; however, in the FRS measurement, the concentration peak occurs 80 K higher than that in the kinetic model. The qualitative shape and differences in concentrations cannot be explained by the uncertainties in the line intensities, detector response, or pressure-broadening coefficient used in the spectral modeling. These observed differences likely arise due to deficiencies in the chemical kinetic model. A path flux analysis of HO_2 formation indicated that at lower-temperature conditions (below 650 K), DME + O_2 → HO_2 + DME radical and H + O_2 + M → HO_2 + M reactions are the dominant formation pathways. This corresponds to the small peak in the HO_2 concentration at around 600 K observed in the chemical kinetic modeling data in Figure 4. At higher-temperature conditions (above 650 K), the dominant formation pathway is the HCO + O_2 → HO_2 + CO reaction. Therefore, the formation of HCO and the uncertainty of HCO + O_2 → HO_2 + CO should be responsible for the discrepancy between the kinetic modeling and experiments. It is known from work by Suzaki et al.[9] that there is a missing HCO formation pathway for DME from QOOH via HOQO not present in the chemical kinetic model that could play a role in the DME chemistry at pressures relevant to the current work. Moreover, a recent high-level calculation by Klippenstein showed that the rate constant of HCO + O_2 → HO_2 + CO predicted by theory is a factor of 2 lower than the rate used in the model between 500 and 1000 K.[21,22] The experimental data in this work confirms that the kinetic model based on the experimental rate overpredicts HO_2 formation and shifts the peak concentration to lower temperature by 80 K. Therefore, quantitative measurements of HCO and HO_2 are important to improve the mechanism prediction.

The current system operates 50 times above the fundamental shot noise limit; therefore, theoretically, it is possible to reduce the detection limit below 100 ppbv under the experimental conditions explored in this work. Excess laser intensity noise due to the low modulation frequency of the electromagnet is the primary limitation. To achieve near-shot-noise performance, a dual modulation scheme could be implemented by performing laser wavelength modulation at frequencies > 10 kHz in addition to the magnetic field modulation (dual modulation FRS).[23] Application of the dual modulation detection method should provide a better sensitivity than the ideal case presented for mid-IR cw-CRDS.

FRS has been successfully used for in situ quantification of HO_2 at the exit of an atmospheric flow reactor. The HO_2 number density was measured by fitting a spectroscopic model to the experimental spectra. The uncertainty in the line intensities represents the largest uncertainty in the obtained HO_2 concentrations. Future studies will focus on the development of a reliable calibration method and remeasurement of the ν_2 band strength. The overall performance of this proof-of-concept system shows the strong potential of FRS as a diagnostic technique for monitoring small gas-phase radicals in combustion processes.

dx.doi.org/10.1021/jz400143c | J. Phys. Chem. Lett. 2013, 4, 872−876

■ ASSOCIATED CONTENT

Supporting Information

The background-subtracted experimental spectra and their corresponding nonlinear model fits are provided. This material is available free of charge via the Internet at http://pubs.acs.org.

■ AUTHOR INFORMATION

Corresponding Author

*E-mail: gwysocki@princeton.edu (G.W.); yju@princeton.edu (Y.J.).

Notes

The authors declare no competing financial interest.

■ ACKNOWLEDGMENTS

This research is partly supported by the Grand Challenges Program of Princeton University. Y.J. would like to thank the support from the Plasma Assisted Combustion MURI research grant from the Air Force Office of Scientific Research and the U.S. Department of Energy, Office of Basic Energy Sciences as part of an Energy Frontier Research Center on Combustion with Grant No. DE-SC0001198.

■ REFERENCES

(1) Curran, H. J.; Gaffuri, P.; Pitz, W. J.; Westbrook, C. K. A Comprehensive Modeling Study of n-Heptane Oxidation. *Combust. Flame* **1998**, *114*, 149−177.

(2) Westbrook, C. K. Chemical Kinetics of Hydrocarbon Ignition in Practical Combustion Systems. *Proc. Combust. Inst.* **2000**, *28*, 1563−1577.

(3) Burke, M. P.; Chaos, M.; Ju, Y.; Dryer, F. L.; Klippenstein, S. J. Comprehensive H_2/O_2 Kinetic Model for High-Pressure Combustion. *Int. J. Chem. Kinet.* **2012**, *44*, 444−474.

(4) Guo, H.; Sun, W.; Haas, F. M.; Farouk, T.; Dryer, F. L.; Ju, Y. Measurements of H_2O_2 in Low Temperature Dimethyl Ether Oxidation. *Proc. Combust. Inst.* **2013**, *34*, 573−581.

(5) Ludwig, W.; Brandt, B.; Friedrichs, G.; Temps, F. Kinetics of the Reaction $C_2H_5 + HO_2$ by Time-Resolved Mass Spectrometry. *J. Phys. Chem. A* **2006**, *110*, 3330−3337.

(6) Bahrini, C.; Herbinet, O.; Glaude, P.-A.; Schoemaecker, C.; Fittschen, C.; Battin-Leclerc, F. Quantification of Hydrogen Peroxide During the Low-Temperature Oxidation of Alkanes. *J. Am. Chem. Soc.* **2012**, *134*, 11944−11947.

(7) Bahrini, C.; Herbinet, O.; Glaude, P.-A.; Schoemaecker, C.; Fittschen, C.; Battin-Leclerc, F. Detection of Some Stable Species During the Oxidation of Methane by Coupling a Jet-Stirred Reactor (JSR) to cw-CRDS. *Chem. Phys. Lett.* **2012**, *534*, 1−7.

(8) Hong, Z. K.; Lam, K. Y.; Sur, R.; Wang, S. K.; Davidson, D. F.; Hanson, R. K. On the Rate Constants of $OH + HO_2$ and $HO_2 + HO_2$: A Comprehensive Study of H_2O_2 Thermal Decomposition Using Multi-Species Laser Absorption. *Proc. Combust. Inst.* **2013**, *34*, 565−571.

(9) Suzaki, K.; Tsuchiya, K.; Koshi, M.; Tezaki, A. Analysis of HO_2 and OH Formation Mechanisms Using FM and UV Spectroscopy in Dimethyl Ether Oxidation. *J. Phys. Chem. A* **2007**, *111*, 3776−3788.

(10) Rothman, L. S.; Gordon, I. E.; Barbe, A.; Benner, D. C.; Bernath, P. F.; Birk, M.; Boudon, V.; Brown, L. R.; Campargue, A.; Champion, J. P.; Chance, K.; Coudert, L. H.; Dana, V.; Devi, V. M.; Fally, S.; Flaud, J. M.; Gamache, R. R.; Goldman, A.; Jacquemart, D.; Kleiner, I.; Lacome, N.; Lafferty, W. J.; Mandin, J. Y.; Massie, S. T.; Mikhailenko, S. N.; Miller, C. E.; Moazzen-Ahmadi, N.; Naumenko, O. V.; Nikitin, A. V.; Orphal, J.; Perevalov, V. I.; Perrin, A.; Predoi-Cross, A.; Rinsland, C. P.; Rotger, M.; Šimečková, M.; Smith, M. A. H.; Sung, K.; Tashkun, S. A.; Tennyson, J.; Toth, R. A.; Vandaele, A. C.; Vander Auwera, J. The HITRAN 2008 Molecular Spectroscopic Database. *J. Quant. Spectrosc. Radiat. Trans.* **2009**, *110*, 533−572.

(11) Westberg, J.; Lathdavong, L.; Dion, C. M.; Shao, J.; Kluczynski, P.; Lundqvist, S.; Axner, O. Quantitative Description of Faraday Modulation Spectrometry in Terms of the Integrated Linestrength and 1st Fourier Coefficients of the Modulated Lineshape Function. *J. Quant. Spectrosc. Radiat. Trans.* **2010**, *111*, 2415−2433.

(12) Gamache, R. R.; Kennedy, S.; Hawkins, R.; Rothman, L. S. Total Internal Partition Sums for Molecules in the Terrestrial Atmosphere. *J. Mol. Struct.* **2000**, *517*−*518*, 407−425.

(13) Welzel, S.; Lombardi, G.; Davies, P. B.; Engeln, R.; Schram, D. C.; Ropcke, J. Trace Gas Measurements Using Optically Resonant Cavities and Quantum Cascade Lasers Operating at Room Temperature. *J. Appl. Phys.* **2008**, *104*, 093115/1−093115/14.

(14) Mercier, X.; Jamette, P.; Pauwels, J. F.; Desgroux, P. Absolute CH Concentration Measurements by Cavity Ring-Down Spectroscopy in an Atmospheric Diffusion Flame. *Chem. Phys. Lett.* **1999**, *305*, 334−342.

(15) Mercier, X.; Therssen, E.; Pauwels, J. F.; Desgroux, P. Cavity Ring-Down Measurements of OH Radical in Atmospheric Premixed and Diffusion Flames. A Comparison with Laser-Induced Fluorescence and Direct Laser Absorption. *Chem. Phys. Lett.* **1999**, *299*, 75−83.

(16) Thiebaud, J.; Crunaire, S.; Fittschen, C. Measurements of Line Strengths in the $2\nu_1$ Band of the HO_2 Radical Using Laser Photolysis/Continuous Wave Cavity Ring-Down Spectroscopy (cw-CRDS). *J. Phys. Chem. A* **2007**, *111*, 6959−6966.

(17) Tang, Y.; Tyndall, G. S.; Orlando, J. J. Spectroscopic and Kinetic Properties of HO_2 Radicals and the Enhancement of the HO_2 Self Reaction by CH_3OH and H_2O. *J. Phys. Chem. A* **2009**, *114*, 369−378.

(18) Zahniser, M. S.; McCurdy, K. E.; Stanton, A. C. Quantitative Spectroscopic Studies of The Hydroperoxo Radical: Band Strength Measurements for The ν_1 and ν_2 Vibrational Bands. *J. Phys. Chem.* **1989**, *93*, 1065−1070.

(19) Kee, R. J.; Rupley, F. M.; Miller, J. A.; Coltrin, M. E.; Grcar, J. F.; Meeks, E.; Moffat, H. K.; Lutz, A. E.; Dixon-Lewis, G.; Smooke, M. D.; Warnatz, J.; Evans, G. H.; Larson, R. S.; Mitchell, R. E.; Petzold, L. R.; Reynolds, W. C.; Caracotsios, M.; Stewart, W. E.; Glarborg, P.; Wang, C.; Adigun, O.; Houf, W. G.; Chou, C. P.; Miller, S. F. *Chemkin Collection*, release 3.7.1; Reaction Design, Inc: San Diego, CA, 2003.

(20) Zhao, Z.; Chaos, M.; Kazakov, A.; Dryer, F. L. Thermal Decomposition Reaction and a Comprehensive Kinetic Model of Dimethyl Ether. *Int. J. Chem. Kinet.* **2008**, *40*, 1−18.

(21) Colberg, M.; Friedrichs, G. Room Temperature and Shock Tube Study of the Reaction $HCO + O_2$ Using the Photolysis of Glyoxal as an Efficient HCO Source. *J. Phys. Chem. A* **2006**, *110*, 160−170.

(22) Klippenstein, S. J. Private Communication; Argonne National Laboratory, Argonne, IL; 2012.

(23) Wang, Y.; Nikodem, M.; Wysocki, G., A. Novel Breath Analyzer for Isotope-Labeled Studies of NO Metabolism. In 2012 International Breath Analysis Meeting, Sonoma, CA, USA, 2012.